AFRL-RX-WP-JA-2015-0035

SHAPE-REPROGRAMMABLE POLYMERS: ENCODING, ERASING, AND RE-ENCODING (POSTPRINT)

M. F. Durstock, R. A. Vaia
AFRL/RXAS

R. R. Kohlmeyer
National Research Council

J. Chen
Dept of Chemistry and Biochemistry, University of Wisconsin-Milwaukee

P. R. Buskohl
UES, Inc.

J. R. Deneault
Universal Technology Corporation

NOVEMBER 2014
Interim Report

AIR FORCE RESEARCH LABORATORY
MATERIALS AND MANUFACTURING DIRECTORATE
WRIGHT-PATTERSON AIR FORCE BASE, OH 45433-7750
AIR FORCE MATERIEL COMMAND
UNITED STATES AIR FORCE

NOTICE AND SIGNATURE PAGE

Using Government drawings, specifications, or other data included in this document for any purpose other than Government procurement does not in any way obligate the U.S. Government. The fact that the Government formulated or supplied the drawings, specifications, or other data does not license the holder or any other person or corporation; or convey any rights or permission to manufacture, use, or sell any patented invention that may relate to them.

This report was cleared for public release by the USAF 88th Air Base Wing (88 ABW) Public Affairs Office (PAO) and is available to the general public, including foreign nationals.

Copies may be obtained from the Defense Technical Information Center (DTIC) (http://www.dtic.mil).

AFRL-RX-WP-JA-2015-0035 HAS BEEN REVIEWED AND IS APPROVED FOR PUBLICATION IN ACCORDANCE WITH ASSIGNED DISTRIBUTION STATEMENT.

//Signature//

MICHAEL F. DURSTOCK
Soft Matter Materials Branch
Functional Materials Division

//Signature//

KATIE E. THORP, Chief
Soft Matter Materials Branch
Functional Materials Division

//Signature//

TIMOTHY J. BUNNING, Chief
Functional Materials Division
Materials and Manufacturing Directorate

This report is published in the interest of scientific and technical information exchange, and its publication does not constitute the Government's approval or disapproval of its ideas or findings.

REPORT DOCUMENTATION PAGE

Form Approved
OMB No. 074-0188

1. REPORT DATE (DD-MM-YYYY)	2. REPORT TYPE	3. DATES COVERED *(From – To)*
November 2014	Interim	05 November 2009 – 17 October 2014

4. TITLE AND SUBTITLE
SHAPE-REPROGRAMMABLE POLYMERS: ENCODING, ERASING, AND RE-ENCODING (POSTPRINT)

5a. CONTRACT NUMBER
In-House

5b. GRANT NUMBER

5c. PROGRAM ELEMENT NUMBER
62102F

6. AUTHOR(S)
(see back)

5d. PROJECT NUMBER
4347

5e. TASK NUMBER

5f. WORK UNIT NUMBER
X03Z

7. PERFORMING ORGANIZATION NAME(S) AND ADDRESS(ES)
(see back)

8. PERFORMING ORGANIZATION REPORT NUMBER

9. SPONSORING / MONITORING AGENCY NAME(S) AND ADDRESS(ES)
Air Force Research Laboratory
Materials and Manufacturing Directorate
Wright Patterson Air Force Base, OH 45433-7750
Air Force Materiel Command
United States Air Force

10. SPONSOR/MONITOR'S ACRONYM(S)
AFRL/RXAS

11. SPONSOR/MONITOR'S REPORT NUMBER(S)
AFRL-RX-WP-JA-2015-0035

12. DISTRIBUTION / AVAILABILITY STATEMENT
Distribution A. Approved for public release; distribution unlimited. This report contains color.

13. SUPPLEMENTARY NOTES
PA Case Number: 88ABW-2014-2998, Clearance Date: 18 June 2014. Journal article published in Advanced Materials 2014, 26, 8114–8119. © 2014 WILEY-VCH Verlag GmbH & Co. KGaA, Weinheim. The U.S. Government is joint author of the work and has the right to use, modify, reproduce, release, perform, display or disclose the work. The final publication is available at DOI: 10.1002/adma.201402901.

14. ABSTRACT
Shape engineering is crucial for controlling the properties and functions of polymers, such as surface roughness, adhesion and wettability, pore size and connection, chirality, and responsiveness towards environmental stimuli, which enable a broad range of applications in microfl uidics, tissue engineering, switchable adhesives, soft robotics, optical devices, and reconfi gurable metamaterials. Conventional plasticshaping techniques like molding depend on complementary replication of the geometry from a physical mold. The cost and time associated with tools and machining used in such a oneto-one linear shape-translation processes often increase rapidly with shape complexity. Additive manufacturing, also called three-dimensional (3D) printing, is a layer-by-layer technology for producing 3D objects directly from a digital model. While 3D printing allows the fabrication of increasingly sophisticated structures on demand, the production time scales signifi cantly with object size. 3D structures of gels and polymers based on bending or swelling have also been fabricated using localized light [13] or heat. Alternatively, non-uniform shape change of heterogeneous multicomponent or multicompartmental materials in response to global environmental stimuli has been exploited to create origami structures. However, the degree of sophistication in applying localized stimuli or fabrication of multicomponent and multicompartmental materials usually correlates with 3D shape complexity.

15. SUBJECT TERMS
programmable shape, reprogrammable, Nafion, shape-memory polymers, shape encoding

16. SECURITY CLASSIFICATION OF:			17. LIMITATION OF ABSTRACT	18. NUMBER OF PAGES	19a. NAME OF RESPONSIBLE PERSON *(Monitor)*
a. REPORT	b. ABSTRACT	c. THIS PAGE			Michael F. Durstock
Unclassified	Unclassified	Unclassified	SAR	10	19b. TELEPHONE NUBER *(include area code)* (937) 255-9208

REPORT DOCUMENTATION PAGE Cont'd

6. AUTHOR(S)

M. F. Durstock, R. A. Vaia - Materials and Manufacturing Directorate, Air Force Research Laboratory, Functional Materials Division
R. R. Kohlmeyer - National Research Council
J. Chen - Department of Chemistry and Biochemistry, University of Wisconsin-Milwaukee
P. R. Buskohl - UES, Inc.
J. R. Deneault - Universal Technology Corporation

7. PERFORMING ORGANIZATION NAME(S) AND ADDRESS(ES)

AFRL/RXAS
Air Force Research Laboratory
Materials and Manufacturing Directorate
Wright-Patterson Air Force Base, OH 45433-7750

National Research Council
Washington, D.C. 20001

Department of Chemistry and Biochemistry
University of Wisconsin-Milwaukee
Milwaukee , Wisconsin 53211

UES, Inc.
Dayton , Ohio 45432

Universal Technology Corporation
Dayton , Ohio 45432

ADVANCED MATERIALS
www.advmat.de

Materials Views
www.MaterialsViews.com

Shape-Reprogrammable Polymers: Encoding, Erasing, and Re-Encoding

Ryan R. Kohlmeyer, Philip R. Buskohl, James R. Deneault, Michael F. Durstock, Richard A. Vaia, and Jian Chen**

Shape engineering is crucial for controlling the properties and functions of polymers, such as surface roughness, adhesion and wettability, pore size and connection, chirality, and responsiveness towards environmental stimuli, which enable a broad range of applications in microfluidics,[1] tissue engineering,[2,3] switchable adhesives,[4–6] soft robotics,[7–9] optical devices,[10,11] and reconfigurable metamaterials.[12] Conventional plastic-shaping techniques like molding depend on complementary replication of the geometry from a physical mold. The cost and time associated with tools and machining used in such a one-to-one linear shape-translation processes often increase rapidly with shape complexity. Additive manufacturing, also called three-dimensional (3D) printing, is a layer-by-layer technology for producing 3D objects directly from a digital model. While 3D printing allows the fabrication of increasingly sophisticated structures on demand, the production time scales significantly with object size. 3D structures of gels and polymers based on bending or swelling have also been fabricated using localized light[13] or heat.[14–16] Alternatively, non-uniform shape change of heterogeneous multicomponent or multicompartmental materials in response to global environmental stimuli has been exploited to create origami structures.[17–19] However, the degree of sophistication in applying localized stimuli or fabrication of multicomponent and multicompartmental materials usually correlates with 3D shape complexity.

Dr. R. R. Kohlmeyer
National Research Council
Washington, D.C. 20001, USA
E-mail: ryan.kohlmeyer.ctr@us.af.mil
Dr. R. R. Kohlmeyer, Dr. P. R. Buskohl, J. R. Deneault, Dr. M. F. Durstock, Dr. R. A. Vaia
Soft Materials Branch, Materials and Manufacturing Directorate
Air Force Research Laboratory
Wright Patterson Air Force Base
Ohio 45433, USA
Dr. R. R. Kohlmeyer, Prof. J. Chen
Department of Chemistry and Biochemistry
University of Wisconsin-Milwaukee
Milwaukee, Wisconsin 53211, USA
E-mail: jianchen@uwm.edu
Dr. P. R. Buskohl
UES, Inc.
Dayton, Ohio 45432, USA
J. R. Deneault
Universal Technology Corporation
Dayton, Ohio 45432, USA

DOI: 10.1002/adma.201402901

Recently, a new shaping strategy has emerged, which prescribes geometric information directly into a single material system via irreversible chemical patterning. Upon exposure to environmental stimuli, the chemical pattern can guide the material undergoing shape transformation from a simple geometry such as a flat sheet into a more-complex 3D structure.[20,21] For example, patterning of a crosslinked region in a planar hydrogel with UV irradiation through a photomask creates a gradient sheet, which undergoes differential swelling or shrinking when exposed to different stimuli.[22,23] In addition, a functional gradient can also be generated by controlling the local orientation of Al_2O_3 platelets in a hydrogel or by photopatterning of the mesogenic unit alignment in a liquid-crystalline polymer network.[24,25] Since the geometric information is embedded permanently, shape-reprogramming of such material systems to achieve unlimited diverse 3D structures from the same piece of polymer is impossible.

Here we report a strategy for shape-reprogramming in a single polymer material, which not only allows shape-encoding and 3D translation of encoded geometric information, but also enables erasing and re-encoding of shape information via reversible localized chemical patterning on the same piece of polymer. Shape-reprogramming refers to the following cyclic process on the same piece of polymer: encoding of 3D shape information via reversible chemical patterning, decoding of encoded 3D shape information via environmental stimuli such as heating without using an external mechanical force or template, erasing of the realized 3D shape via chemical treatment and heating, then re-encoding different 3D shape information with another chemical pattern. In essence, our shape-reprogrammable polymer (SRP) acts as computer hardware that can be reformatted and reprogrammed repeatedly. Hence, a single piece of SRP is sufficient, in principle, to produce numerous complex 3D shapes that are prescribed in simple chemical patterns.

Shape-memory polymers (SMPs) are materials that can memorize one or multiple temporary shapes and are able to return from this temporary shape to their permanent shape upon exposure to an external stimulus such as heat.[6,26–29] Nafion is a commercially available SMP with a multi-shape-memory effect.[6,29,30] Recently, we reported[15] that any shape of Nafion or its composite can be reversibly locked and unlocked with high fidelity by deprotonation and reprotonation, respectively (**Figure 1**). Chemical locking is particularly useful for stabilizing temporary shapes against heating to temperatures at or higher than the initial deformation temperature (T_{def}), the temperature at which a film was stretched before shape-fixing

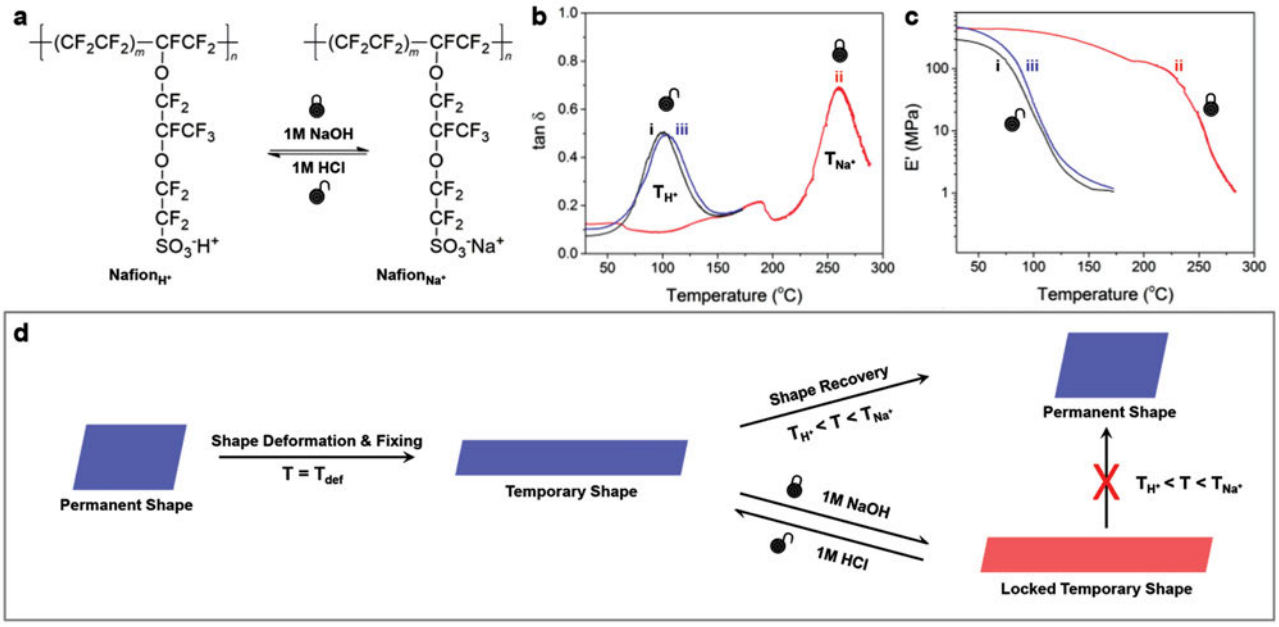

Figure 1. Overview of shape-locking and unlocking of Nafion. a) Nafion chemical structure and the reversible chemistry between the protonated (unlocked) and deprotonated (locked) forms. Nafion is a commercial thermoplastic polymer that possesses a low degree of crystallinity. These crystals serve as physical crosslinks that prevent flow above the thermal relaxation temperatures, as well as hold a temporary shape during the shape-memory process.[29] b,c) DMA curves of (b) tan δ and (c) storage modulus E' of: i) an unlocked Nafion film, ii) a locked film obtained from 1 M NaOH treatment of (i), and iii) a recovered unlocked film obtained from 1 M HCl treatment of (ii). d) The unlocked Nafion film exhibits the typical shape-memory effect and undergoes shape-recovery upon heating above T_{def} and between the onset of T_{H^+} and T_{Na^+}, whereas the locked Nafion temporary shape remains stable.

upon cooling.[15] Studying the thermal relaxations of these two distinct phases using dynamic mechanical analysis (DMA) has been well documented.[31] Our results of protonated, deprotonated, and re-protonated Nafion confirms the dramatic increase, as well as recovery, of the temperature of cooperative thermal relaxation from 100 (T_{H^+}) to 260 °C (T_{Na^+}) (Figure 1b,c). Here, Nafion is locked (deprotonated) by immersion in 1 M NaOH, and unlocked (re-protonated) by immersion in 1 M HCl. At temperatures between the onset of T_{H^+} and T_{Na^+}, the locked phase (Nafion$_{Na^+}$) is mechanically stiffer than the unlocked phase (Nafion$_{H^+}$). As such, the unlocked phase uniquely exhibits a shape-memory effect when heated to these intermediate temperatures (Figure 1d).

Shape-patterning and reprogramming exploits this reversible acid–base, chemically induced shift in relaxation temperature. Both phases can be patterned within a Nafion film via local deposition of a deprotonation ink (NaOH). Differential shrinking between these coexisting regions occurs upon heating causing the originally planar film to transform to a 3D conformation that is precisely dictated by the pattern of locked–unlocked phases. Since the acid–base chemistry is fully reversible, chemical patterning of shape-memory and locked-shape-memory phases can be encoded, erased, and re-encoded, repeatedly, in a single piece of Nafion (see Experimental Section and Supporting Information for details).

To simplify the discussion, "heating" will specifically refer to treating the film to temperatures greater than T_{def} and between the onset of T_{H^+} and T_{Na^+}. We first demonstrate the 3D shaping capability of our system by patterning a uniaxially stretched Nafion film. Without locking treatment, the film uniaxially shrinks upon heating, completely recovering its original shape, whereas a film completely locked in its temporary shape remains unchanged upon heating (Figure 1d and Supporting Information, Figure S1). In contrast, heating a film patterned with a short line of locked material parallel to the stretching direction leads to bending of the strip toward the patterned surface (**Figure 2**a,b and Supporting Information, Figure S2d–g). Bending suggests the presence of a gradient in locking through the thickness of the film. This was confirmed by energy-dispersive X-ray spectroscopy (EDS), which showed a deprotonated area on the bottom of the film approximately 10% larger relative to the top (Supporting Information, Figure S3,S4). Also, infrared (IR) spectroscopy showed a similar chemical transformation on both sides of the locked region indicating both surfaces were locked through the thickness (Supporting Information, Figure S5). In concert, finite element (FE) modeling verifies that upward bending requires a larger area of locking on the bottom of the film relative to the top surface where the NaOH ink was applied (Supporting Information, Figure S6,S7). With a larger locked footprint on the bottom, the film contracts more on the top and consequently forms an upward bend (Figure 2c and Supporting Information, Figure S7d). This direct coupling between the mechanics and the chemical profile provide a powerful framework to control the direction and shape of 3D structures. The locking gradient is sensitive to diffusion-related variables, such as the applied NaOH concentration, the treatment time, and the film thickness. For example, by decreasing the reagent volume over the same pattern area, and thus decreasing the extent of the de-protonation gradient, the film bends downward, reflecting more contraction (i.e. less locking) on the bottom surface (Supporting Information, Figure S7c, S8f–j).

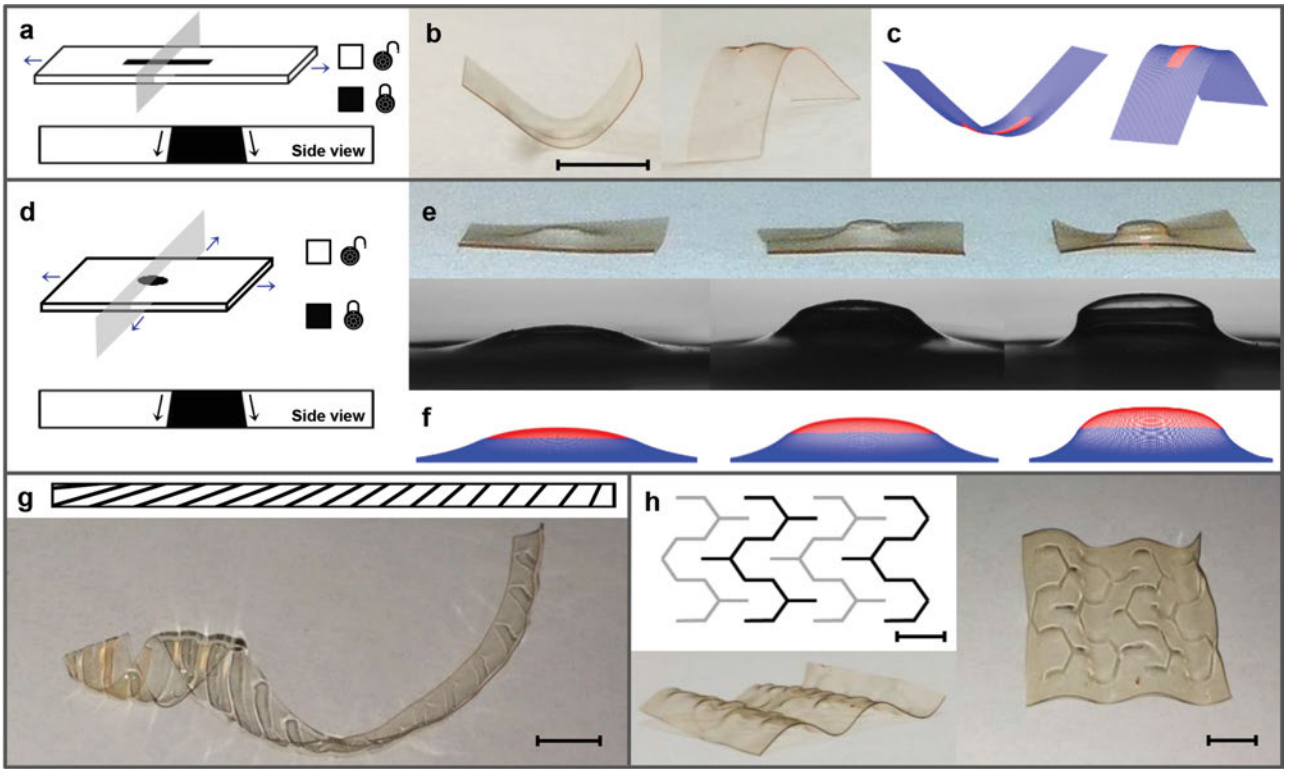

Figure 2. Overview of shape-encoding and decoding of uniaxially stretched (*us*-) and biaxially stretched (*bs*-) Nafion$_{SRPs}$. a) Schematic representation of a *us*-Nafion$_{SRP}$ with a patterned line (the blue arrows indicate the stretching direction). b) Photographs of a *us*-Nafion$_{SRP}$ (stretched to $\varepsilon = 33\%$ at 120–130 °C), which was patterned with a 1.5 µL line of 1 M NaOH, then heated at 120–130 °C for 30 s (patterned side up on left and down on right). c) FE model of *us*-Nafion$_{SRP}$ after encoding and decoding. d) Schematic representation of *bs*-Nafion$_{SRP}$ with a patterned dot. e) Photographs of 5 mm square films (patterned side down) after patterning with a 0.5 µL dot of 1 M NaOH and heating for 5 min at 130 °C. Before patterning, the films were stretched using a biaxial stretching device at 120–130 °C to various strains (left: $\varepsilon = 20\%$, middle: $\varepsilon = 62\%$, right: $\varepsilon = 125\%$). f) FE models of the *bs*-Nafion films with 5%, 10%, and 20% shrinkage upon heating. g) Scheme of dynamic right-handed helix locking pattern and photograph of *us*-Nafion$_{SRP}$ (stretched to $\varepsilon = 49\%$ at 120–130 °C) that was patterned at a angles varying from 10–60° with 1.5–2.0 µL of 1 M NaOH per line, then heated at 120–130 °C (resting in a polytetrafluoroethylene (PTFE) dish for 5 min, followed by hanging from a clip for 1 min). h) Pattern printing. Computer-aided design (CAD) scheme of locking pattern with lines patterned on the top (black) and bottom (gray) of the film, and photographs after patterning a *us*-Nafion$_{SRP}$ ($\varepsilon = 54\%$) by printing with 1 M NaOH with 5% (v/v) ethylene glycol, then heating for 5 min at 130 °C. Scale bars: 0.5 cm.

By controlling the size, location, and orientation of the patterns in a flat sheet, complex 3D shapes with positive and negative deflections can be prescribed on pre-stretched Nafion films. For instance, arbitrary helical shapes can be produced with predictive and precise control of helical handedness, radius, and pitch distance (Figure 2g and Supporting Information, Figure S9–S11). These macroscopic helical structures mimic some of those found in nature, which can be seen in seashells, horns, plant tendrils, and seed pods.[32] Alternatively, zigzag structures could be created with a similar degree of control by patterning on both sides of the film (Supporting Information, Figure S12). Since the shape-encoding chemistry is fully reversible, it is possible to convert a zigzag shape to a right-handed helix by shape-reprogramming of the same rectangular sheet of Nafion directly (Supporting Information, Figure S13).

A biaxially stretched Nafion film with circular dot patterning experiences buckling in the locked area, as well as shrinking in the unlocked area in response to heating, which leads to the formation of dome structures that resemble the profile of a 3D Gaussian shape (Supporting Information, Figure S2a–c, S14). By changing the film stretch ratios, various dome shapes can be created (Figure 2e). In all cases, the buckling direction is towards the bottom side of the film due to a smaller locked area on the top of the film (Figure 2d), as confirmed by FE modeling (Figure 2f). Following from the mechanical analysis, a group of domes with controlled size and location can be produced by printing a pattern of dots on a biaxially stretched Nafion film using a plotter equipped with a 30 µm felt-tip pen (Supporting Information, Figure S14g). Alternatively a 3D textured wave structure could be generated with a series of patterned lines by printing on both sides of a uniaxially stretched Nafion film using the same plotter equipped with a 200 µm felt-tip pen (Figure 2h). Inkjet printing, aerosol jet printing, masked aerosol spray-coating, and microcontact printing with a rolling stamp will allow for rapid, large-area printing of arbitrary patterns with a hierarchy of length scales tunable for each application.

The reversibility of the deprotonation–protonation chemistry further enhances the versatility of SRPs so that the same strip of film can be repurposed and reprogrammed into multiple 3D shapes. For example, **Figure 3** summarizes the sequential reprogramming of Nafion using three different encoding methods: a zigzag prescribed in a uniaxially

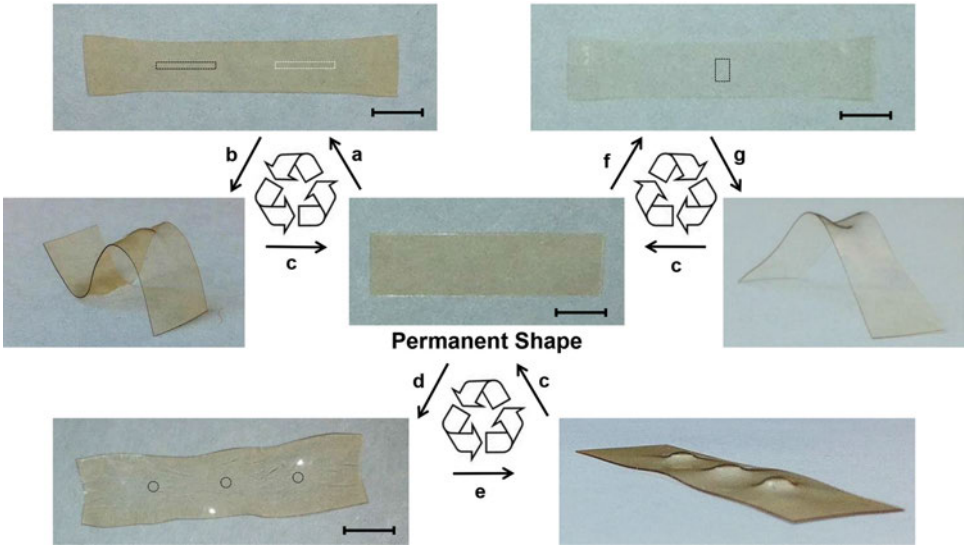

Figure 3. Shape-reprogramming. a) Room-temperature uniaxial hand stretching to $\varepsilon = 33\%$ and then patterning with two 1.5 μL lines of 1 M NaOH (the black rectangle represents the top side and the white rectangle represents the bottom side). b) Heating of patterned film by hanging for 30 s at 120 °C. c) Soaking film in 1 M HCl for 20 min followed by heating for 1 min at 120 °C to recover the permanent shape. d) Room-temperature biaxial hand stretching to $\varepsilon = 20\%$ in the *x* and *y* directions and then patterning with three 0.5 μL dots of 1 M NaOH (the pattern shown with black circles). e) Heating of patterned film in a PTFE dish for 5 min at 120 °C. f) Room-temperaure uniaxial hand stretching to $\varepsilon = 39\%$ followed by complete locking by soaking in 1 M NaOH for 1 h and then patterning with 5 μL of 1 M HCl. g) Heating of patterned film in a PTFE dish for 10 min at 150 °C. Scale bars: 0.5 cm.

stretched film with line patterning, domes prescribed in a biaxially stretched film with dot patterning, and a bend with a saddle shape prescribed in a locked uniaxially stretched film with reverse patterning (Figure 3). In reverse patterning, localized addition of 1 M HCl to a fully locked Nafion temporary shape leads to a Nafion film with patterned unlocked regions (Figure 3 and Supporting Information, Figure S15). This reverse-patterning example enables bending, but retains the rigid facets of the locked Nafion, which could be more useful for applications in origami engineering.

Finally, the general shape-reprogramming methodology is not restricted to initially flat substrates. For example, heat-induced differential shrinkage dictated by simple chemical patterns on seamless Nafion tubing gives rise to prescribed complex tubing shapes with modulated radius, helicity, and surface morphology (**Figure 4** and Supporting Information,

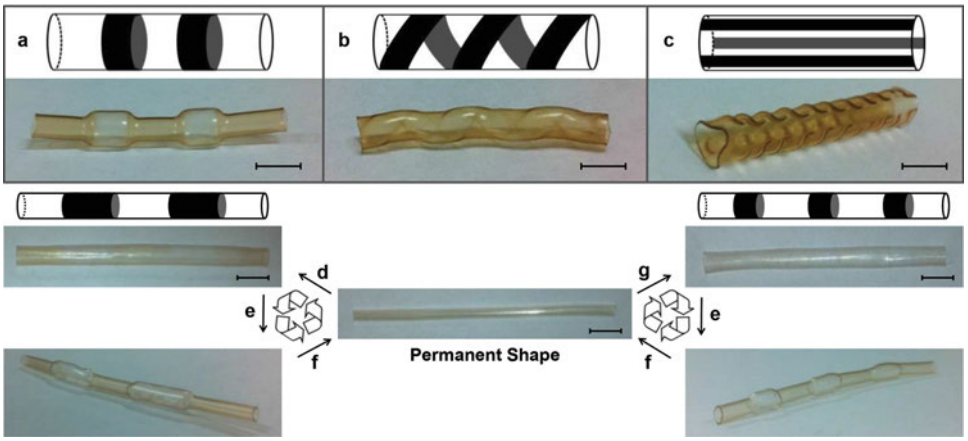

Figure 4. 3D shaping and reprogramming of Nafion tubing. a–c) Schemes of three different locking patterns and photographs of corresponding 3D-shaped tubes after removing the patterned tube from the awl and heating in a PTFE dish. a) Two 4-mm-wide strips of NaOH-soaked paper towel were wrapped around the tube. The encoded tube was heated at 140 °C for 10 min. b) A 3-mm-wide strip of NaOH-soaked paper towel was wrapped around the tube. The encoded tube was heated at 150 °C for 10 min. c) Three 3-mm-wide strips of NaOH-soaked filter paper were rested across the tube. The encoded tube was heated at 140 °C for 10 min. d–g) Shape-reprogramming of Nafion tubing. d) Radial stretching followed by patterning with two 8-mm-wide strips of NaOH-soaked paper towel that were wrapped around the tube. Corresponding scheme of the locking pattern is shown above. e) Heating of encoded tube at 140 °C for 2 min. f) Soaking film in 1 M HCl for 20 min followed by heating at 140 °C for 10 min to recover the permanent shape. g) Radial stretching followed by patterning with three 4-mm-wide strips of NaOH-soaked paper towel that were wrapped around the tube. Corresponding scheme of the locking pattern is shown above. Scale bars: 0.5 cm.

Figure S16). As with the films, the same tubing can be reprogrammed from one 3D shape to another by encoding, erasing, and re-encoding of shape information via through-thickness chemical patterning of the tube's surface (Figure 4d–g). Such sophisticated 3D tubing geometries with any length are either difficult or impossible to make via other shaping methods. The ability to rationally engineer tubing morphology allows fine control of gas and fluidic transport for targeted applications such as controlled mixing (Figure 4a), vortex flow (Figure 4b), or decelerated flow (Figure 4c).

In conclusion, shape-reprogramming of shape-memory polymers represents an exciting new strategy to develop re-useable, sustainable materials for morphing technologies ranging from medical implants and lab-on-a-chip, to robotics and satellite deployment. The key to this methodology is accessible and reversible acid–base chemistry that shifts the softening temperature of a shape-memory polymer. The demonstration of reprogramming with Nafion is potentially amenable to other ionomers with sulfonic acid or carboxylic acid groups, as well as other polymers that can undergo reversible side-chain crosslinking such as cycloaddition or supramolecular reactions.[33–36] Overall, SRPs provide an avenue to engineering arbitrary complex forms that morph to enable complex functions. Future studies include the development of new SRP materials, printing patterns to achieve even-more-complex 3D shape outputs, as well as developing a computational topology optimizer that can directly predict an input pattern for a desired 3D output shape.

Experimental Section

Nafion N115 films (DuPont, t = 127 μm) were purchased through Ion Power, Inc. All as-received Nafion_{H^+} films were annealed at 140 °C for 2 h to reach their equilibrium states. The stretch ratio, λ, as used throughout this work is defined as $\lambda = (L/L_0)$, where L_o is the initial length of the film and L is the final length of the film after stretching. The strain, ε, is defined by $\varepsilon = 100\% \times (L - L_0)/L_0$.

Chemical locking refers to the process of converting Nafion_{H^+} to Nafion_{Na^+} or Nafion_{K^+} by a selective treatment with a 1 M NaOH or KOH solution. Selective locking treatments were done using a 0.5–10 μL micropipetter, and the locking pattern was wiped away using paper towel before drying. Unless otherwise specified, all locking reagent patterns were left on the film for 10 s, then wiped away with a paper towel. Chemical unlocking for shape-reprogramming experiments refers to the process of converting the Nafion_{Na^+} or Nafion_{K^+} regions back to Nafion_{H^+} by soaking in a 1 M HCl solution for 20 min, followed by washing with deionized water. The original permanent shape was recovered by heating the unlocked material for 1 min at 120 °C. Nafion tubing for 3D shaping experiments was purchased through Perma Pure LLC (model numbers TT-110 and TT-070). Printing of locking patterns was accomplished using a Graphtec FC2250 plotter fitted with a Copic 30 μm or 200 μm felt-tip pen. The patterns were prepared using TurboCAD Deluxe 20.0 and exported as Drawing eXchange Format (.DXF) to be read by the plotter. Additional details of 3D-shaping and reprogramming experiments are described in the figure captions in both the text and the Supporting Information.

Sample Characterization: Dynamic mechanical analysis (DMA) measurements were acquired using a TA Instruments DMA Q800 under nitrogen. Samples were run in tensile mode at a frequency of 1 Hz and a heating rate of 3 °C min^{-1}. 1 MPa was used to determine the lower modulus limit of each run. For unlocked samples, going above the temperature associated with this modulus (ca. 175 °C) caused the sample to become very soft or rip, which caused the data to become noisy and unreliable. Measurements were recorded after first heating a sample up to 130 °C inside the DMA instrument and cooling back down to 30 °C to remove residual moisture in the sample. Energy dispersive X-ray spectroscopy (EDS) mapping was run using a FEI Quanta 600F scanning electron microscope (SEM) equipped with an EDAX Ametek Octane Super detector. EDS mapping was performed at a 30 kV accelerating voltage and a 50× magnification using EDAX TEAM Enhanced V4.0.0 software. All the maps were collected using the high-quality mapping setting, which took ca. 30 min at a count rate of 40 000 counts per second. For each sample, 0.5 μL of 1 M KOH was placed on the top of each Nafion film and wiped away before drying. EDS maps of both sides of each sample were taken immediately after wiping KOH away. The EDS map of the bottom of the film (opposite to the patterned side) was always acquired before the top of the film (pattered side). Yellow circles were drawn around the outline of the potassium regions and the areas of each spot were measured using ImageJ 1.45s software. Attenuated total reflectance-FTIR (ATR-FTIR) spectra were obtained via a Bruker ALPHA FT-IR spectrometer equipped with an ALPHA-P diamond ATR module.

Mechanical Modeling: Finite element (FE) modeling was employed to determine how patterned locking was capable of generating a bending response in the *us*-Nafion film. A rectangular geometry, as shown in Figure 2a, was discretized with 4-node, two-layer shell elements in the commercial FE package ANSYS. The initial, undeformed configuration in the model corresponded to the stretched state in the experiment. To simulate the contraction along the stretching direction, an isochoric deformation was prescribed throughout the model using anisotropic coefficients of thermal expansion. In this way, the temperature field throughout the model acted as the load parameter for the magnitude of the axial contraction (Supporting Information, Figure S6a). To ensure that the prescribed deformation was volume preserving ($\det(\mathbf{F}_{us}) = 1$), we assume that for the uniaxial case the deformation gradient was $\mathbf{F}_{us} = \text{diag}(\lambda, \lambda^{-1/2}, \lambda^{-1/2})$. Hence, as the axial direction shrinks with increasing load parameter, the orthogonal y and z directions expand (Supporting Information, Figure S6a). The same approach was applied to the *bs*-Nafion films, with an assumed deformation gradient of $\mathbf{F}_{bs} = \text{diag}(\lambda, \lambda, \lambda^{-2})$. Apart from the thermal-expansion coefficients, all the other material properties were isotropic. We assumed a linear elastic material model for the Nafion films. Young's modulus was E_{H^+} = 200 MPa in the unlocked regions and E_{Na^+} = 400 MPa in the locked regions. We used the load parameter, T (temperature) to also assign the stiffness of the locked (T = 0) and unlocked regions ($T \geq 0.03$), respectively (Supporting Information, Figure S6b). A nearly incompressible Poisson's ratio of $\nu = 0.499$ was assigned to all regions.

Supporting Information

Supporting Information is available from the Wiley Online Library or from the author.

Acknowledgements

R.R.K. thanks the National Research Council for the Postdoctoral Fellowship. The authors thank A. Safriet for helping to design and machine the biaxial stretching device. The authors acknowledge helpful discussions with A. Schwabacher.

Received: June 30, 2014
Revised: August 21, 2014
Published online: October 17, 2014

[1] M. Jamal, A. M. Zarafshar, D. H. Gracias, *Nat. Commun.* **2011**, *2*, 527.
[2] M. E. Kolewe, H. Park, C. Gray, X. Ye, R. Langer, L. E. Freed, *Adv. Mater.* **2013**, *25*, 4459.

[3] G. Villar, A. D. Graham, H. Bayley, *Science* **2013**, *340*, 48.
[4] A. Sidorenko, T. Krupenkin, A. Taylor, P. Fratzl, J. Aizenberg, *Science* **2007**, *315*, 487.
[5] B. Pokroy, S. H. Kang, L. Mahadevan, J. Aizenberg, *Science* **2009**, *323*, 237.
[6] T. Xie, *Polymer* **2011**, *52*, 4985.
[7] F. Ilievski, A. D. Mazzeo, R. F. Shepherd, X. Chen, G. M. Whitesides, *Angew. Chem. Int. Ed.* **2011**, *50*, 1890.
[8] S. A. Morin, R. F. Shepherd, S. W. Kwok, A. A. Stokes, A. Nemiroski, G. M. Whitesides, *Science* **2012**, *337*, 828.
[9] R. R. Kohlmeyer, J. Chen, *Angew. Chem. Int. Ed.* **2013**, *52*, 9234.
[10] N. Bowden, S. Brittain, A. G. Evans, J. W. Hutchinson, G. M. Whitesides, *Nature* **1998**, *393*, 146.
[11] H. Xu, C. Yu, S. Wang, V. Malyarchuk, T. Xie, J. A. Rogers, *Adv. Funct. Mater.* **2013**, *23*, 3299.
[12] N. I. Zheludev, Y. S. Kivshar, *Nat. Mater.* **2012**, *11*, 917.
[13] J. Ryu, M. D'Amato, X. Cui, K. N. Long, H. J. Qi, M. L. Dunn, *Appl. Phys. Lett.* **2012**, *100*, 161908.
[14] Y. Liu, J. K. Boyles, J. Genzer, M. D. Dickey, *Soft Matter* **2012**, *8*, 1764.
[15] R. R. Kohlmeyer, M. Lor, J. Chen, *Nano Lett.* **2012**, *12*, 2757.
[16] C. Yu, Z. Duan, P. Yuan, Y. Li, Y. Su, X. Zhang, Y. Pan, L. L. Dai, R. G. Nuzzo, Y. Huang, H. Jiang, J. A. Rogers, *Adv. Mater.* **2013**, *25*, 1541.
[17] L. Ionov, *Soft Matter* **2011**, *7*, 6786.
[18] K.-U. Jeong, J.-H. Jang, D.-Y. Kim, C. Nah, J. H. Lee, M.-H. Lee, H.-J. Sun, C.-L. Wang, S. Z. D. Cheng, E. L. Thomas, *J. Mater. Chem.* **2011**, *21*, 6824.
[19] K. J. Lee, J. Yoon, S. Rahmani, S. Hwang, S. Bhaskar, S. Mitragotri, J. Lahann, *Proc. Natl. Acad. Sci. USA* **2012**, *109*, 16057.
[20] Y. Klein, E. Efrati, E. Sharon, *Science* **2007**, *315*, 1116.
[21] E. Sharon, E. Efrati, *Soft Matter* **2010**, *6*, 5693.
[22] J. Kim, J. A. Hanna, M. Byun, C. D. Santangelo, R. C. Hayward, *Science* **2012**, *335*, 1201.
[23] H. Thérien-Aubin, Z. L. Wu, Z. Nie, E. Kumacheva, *J. Am. Chem. Soc.* **2013**, *135*, 4834.
[24] R. M. Erb, J. S. Sander, R. Grisch, A. R. Studart, *Nat. Commun.* **2013**, *4*, 1712.
[25] K. M. Lee, T. J. Bunning, T. J. White, *Adv. Mater.* **2012**, *24*, 2839.
[26] P. T. Mather, X. Luo, I. A. Rousseau, *Annu. Rev. Mater. Res.* **2009**, *39*, 445.
[27] M. Behl, M. Y. Razzaq, A. Lendlein, *Adv. Mater.* **2010**, *22*, 3388.
[28] S. A. Madbouly, A. Lendlein, *Adv. Polym. Sci.* **2010**, *226*, 41.
[29] G. J. Berg, M. K. McBride, C. Wang, C. N. Bowman, *Polymer* **2014**, DOI: 10.1016/j.polymer.2014.07.052.
[30] T. Xie, *Nature* **2010**, *464*, 267.
[31] K. A. Page, K. M. Cable, R. B. Moore, *Macromolecules* **2005**, *38*, 6472.
[32] Y. Forterre, J. Dumais, *Science* **2011**, *333*, 1715.
[33] A. Lendlein, H. Jiang, O. Jünger, R. Langer, Nature **2005**, *434*, 879.
[34] J. Li, J. A. Viveros, M. H. Wrue, M. Anthamatten, *Adv. Mater.* **2007**, *19*, 2851.
[35] C. J. Kloxin, C. N. Bowman, *Chem. Soc. Rev.* **2013**, *42*, 7161.
[36] K. Liu, Y. Kang, Z. Wang, X. Zhang, *Adv. Mater.* **2013**, *25*, 5530.